Cryogenic Refrigeration Systems as an Enabling Technology in Space Sensing Missions

T. Roberts and F. Roush

Air Force Research Laboratory AFRL/VSSS
Kirtland AFB, NM 87117

ABSTRACT

Infrared (IR) space sensing missions of the future depend upon low mass, and highly capable imaging technologies. Limitations in visible imaging due to the earth's shadow drive the use of IR surveillance methods for a wide variety of applications for Intelligence, Surveillance, and Reconnaissance (ISR) or for Ballistic Missile Defense (BMD) applications. Utilization of IR sensors greatly expands and improves mission capabilities including target and target behavioral discrimination. Background IR emissions and electronic noise that is inherently present in Focal Plane Arrays (FPAs) and surveillance optics bench designs obviates their use unless they are cooled to cryogenic temperatures. This paper describes the role of cryogenic coolers as an enabling technology for generic ISR and BMD missions and provides ISR and BMD mission and requirement planners with a brief glimpse of this critical technology implementation potential. Practical alternatives to active refrigeration systems for certain mission types are also described. The interaction between cryogenic refrigeration component performance and the IR sensor optics and FPA can be seen as not only mission enabling but also as mission performance enhancing when the refrigeration system is considered as part of an overall optimization problem.

INTRODUCTION

It should be noted as a preliminary that sensing targets can either be observed using their reflected or emitted radiation. During the past six decades infrared (IR) detector systems have been explicitly tied to cryogenic refrigeration, as discussed in Ross.[1] This has been due in large part to cryogenic refrigeration being an absolute requirement for many of these detectors to work. The situation in space situational awareness (SSA) or intelligence, surveillance, and reconnaissance (ISR), or astronomy applications differs greatly from the case of terrestrial or avionic applications, principally due to the isolation of those applications from any source of maintenance or replenishment of working fluids. During these decades, cryogenic refrigeration in space has matured from a difficult potential to a flexible resource enabling detectors to not just work, but to also support general needs to reduce payload mass and power consumption.

DETECTOR THERMAL INTERACTIONS

The principal types of IR detectors have been described comprehensively[2], but this discussion will be centered upon a relative few that have been qualified for detecting targets of military interest, see Figure 1 and Table 1.

Cryocoolers 14, edited by S.D. Miller and R.G. Ross, Jr.

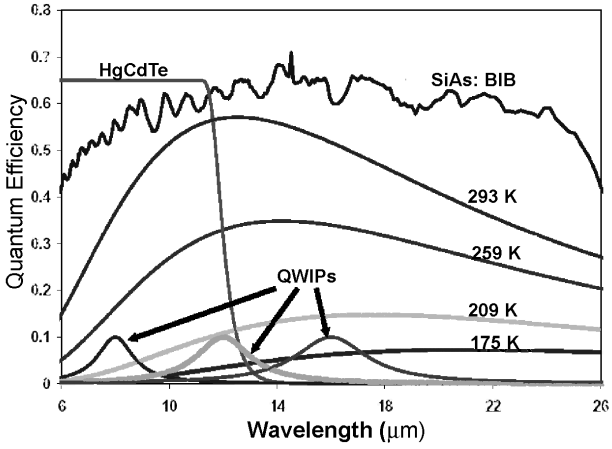

Figure 1. Comparative FPA performance in the MW-VLWIR spectrum versus relative emissivity of blackbodies at indicated temperatures.

Table 1. Operational Ranges of Selected FPA Materials

Material	Spectral band (micron)	Operating temperature (K)
Si	<1	300
PtSi	1-5	60-90
InSb	<6	35-90
PbSe	1-5	220
HgCdTe SWIR	<3	150-220
HgCdTe MWIR	2-6	100-120
HgCdTe LWIR (low background)	6-14	35-40
Si:As	6-28	8-12
QWIPs	various l micron bands	40-80
PbS	1-3	220-300

It should be noted that Table 1 includes several detector materials which have wide use in avionic and terrestrial applications, or have been used in the past in space. Today, most space applications use amorphous silicon in the visible band, various alloy compositions of HgCdTe in the SWIR through LWIR bands, or Si:As for the VLWIR (through MWIR) band. Increased interest in various wide-field, scanning applications is based upon the availability of InSb and HgCdTe in array sizes of over 4 million pixels operating in the SWIR and MWIR bands. First, the detector system must be cooled below its maximum operating temperature, as indicated in Table 1. Second, the operating noise of the detector itself must be reduced to a fraction of the array's dynamic output, usually below a figure of one sixth of the anticipated output of the detector when it is viewing an average target. This operating noise comes from several sources in the detector, many thermally induced, and is called "dark current". The net effect of "dark current" in reducing detector sensitivity can be seen in Figure 2.[3]

Detector cooling also enables the use of wider-band or more capable focal plane arrays. Figure 3 indicates how higher temperature HgCdTe alloys can address many SWIR through LWIR bands, but the overall performance of Si:As is superior to HgCdTe in any band longer than the SWIR.[4] The relatively narrow response range of QWIP arrays is also shown. The net effect of this interaction between detector and refrigeration capacity is shown in Figures 4 and 5. The superior performance of the larger bandwidth Si:As is partially due to its high sensitivity and also due to its more comprehensive bandwidth when used in a noise-limited detector. The ability to discern a target from clutter in the noise-limited case is a direct effect of detector signal-to-noise ratio, and as Figure 5 shows, the detector not only sees a target more sharply but also suppresses clutter stemming from detector noise and the scene background.[5]

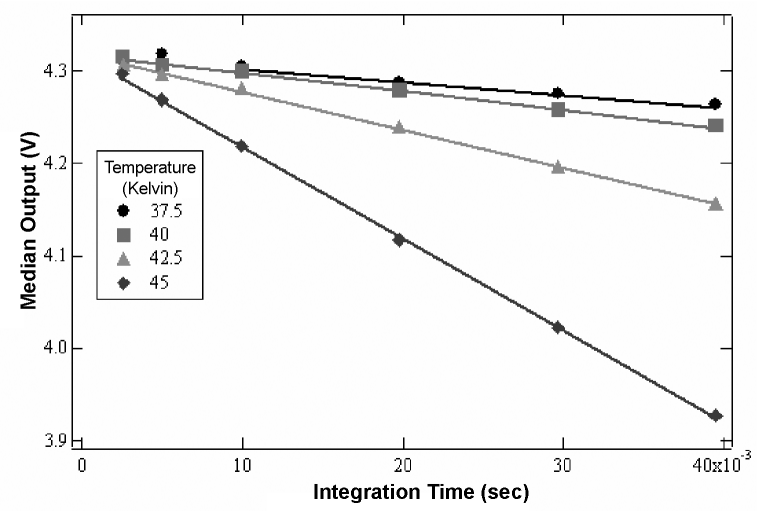

Figure 2. Median output versus integration time at various temperatures for a LWIR HgCdTe FPA.

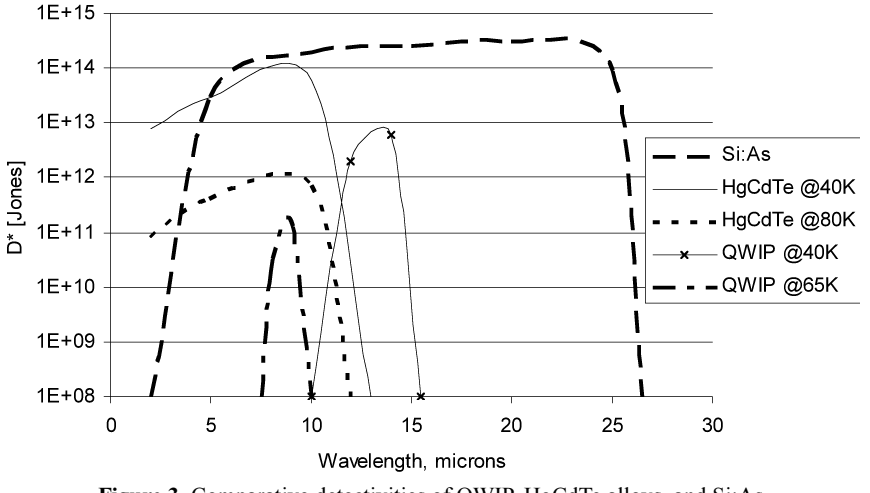

Figure 3. Comparative detectivities of QWIP, HgCdTe alloys, and Si:As.

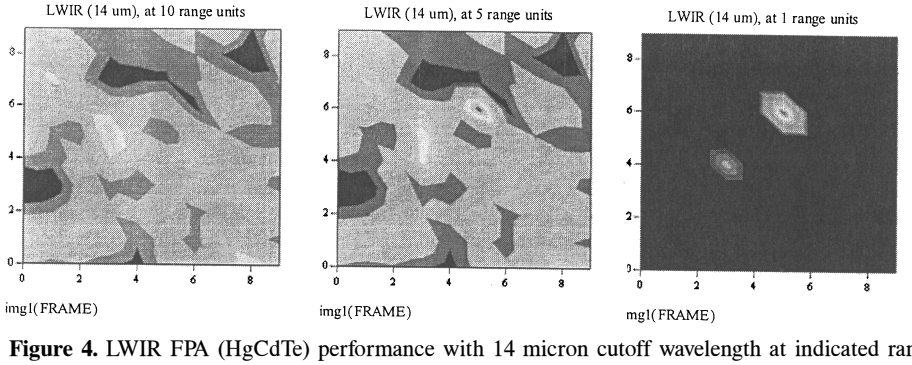

Figure 4. LWIR FPA (HgCdTe) performance with 14 micron cutoff wavelength at indicated range units. The lower target is at 240 K, and the upper is at 300 K.

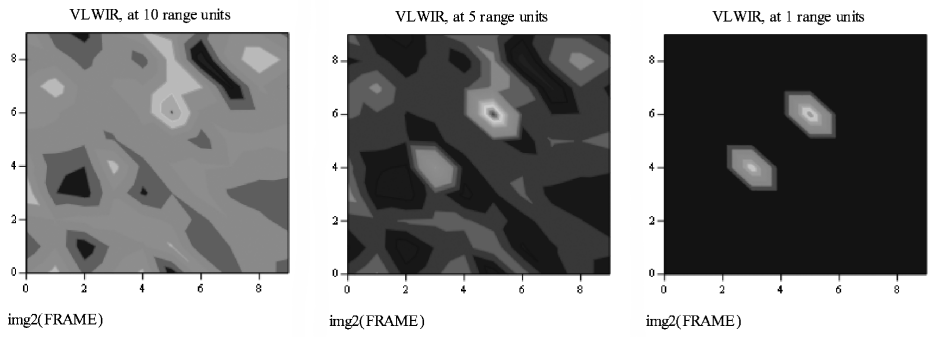

Figure 5. LWIR FPA (Si:As) performance with 28 micron cutoff, same targets as Figure 5.

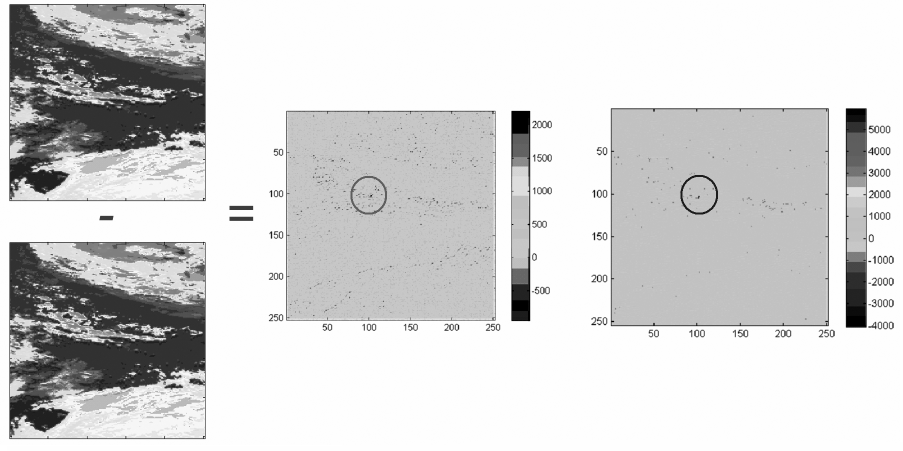

Figure 6. Background limited SWIR/MWIR scene with fast moving targets and ground clutter. Temporal subtraction yields middle frame and spatial difference algorithms gives right frame. The targets of interest are circled.

The case alters with background limited scenes, as the scene noise and clutter will have approximately the same intensity, as they are far larger than the internal noise in the detector. The use of temporal and spatial filtering to discern targets of interest is shown in Figure 6. Further discrimination can be obtained by use of two or more color bands to show how the target's reflected or emitted signature differs significantly from its background or decoys.[6]

CRYOGENIC REFRIGERATION'S ROLE IN DETECTOR OPERATION

Asides from the near impossibility of detecting the infrared signature of something that is colder than the detector, active refrigeration becomes critical to mission success for several reasons. As mentioned above, certain materials simply don't function above critical temperatures. But the optimal operating condition for any of these has little to do with the emission peaks in Figure 1, related directly to the target and environment seen by the detector. Therefore, in order to see distant and dim targets, even visible or ultraviolet light detectors may have to be cooled in order to increase their signal-to-noise ratio. This issue is moot in the background-limited case (as the background noise predominates over the detector noise), but in the usual case of space situational awareness in which distant moving objects do not have bright backgrounds, greater cooling loads and lower temperatures are beneficial. It should be noted that in this case, the use of the astronomers' method of very long integration times and low frame rates is restricted by the moving nature of such targets.

This benefit is reinforced by the need for detector calibration. In any detector array the voltage output of the detector can be estimated as a linear function of photon incidence, in which the slope

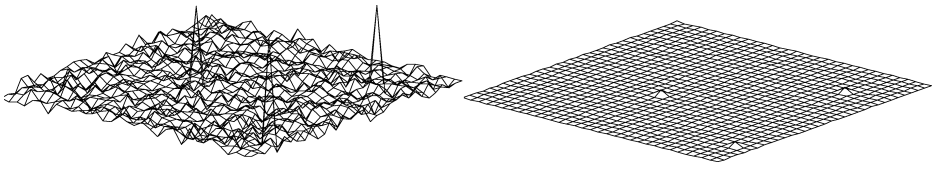

Figure 7. Non-calibrated detector output vs. calibrated output.

of the function is the pixel detection gain and the intercept its calibration offset at no radiative incidence. By measuring pixel responses with respect to a known source intensity and complete darkness, the output of any pixel can be normalized, assuming that its linearization function is within certain bounds. Figure 7 shows the dramatic impact of array clibartion on output uniformity.[5]

It is important to note that this calibration is valid for a certain temperature band about the calibration temperature. If a detector's temperature is allowed to vary temporally, on a pixel by pixel basis, then its calibration is invalid to some degree or another. Just how invalid the output of a thermally unstable detector would be is extremely difficult to predict or even measure during continuous missions. Also, it is virtually impossible to measure the temperature of each pixel, as opposed to some representative temperature near the FPA. Consequently, the standards for most mission's detector stability are simply expressed as 0.1 K above or below the calibration temperature at all times. For a small detector, with a relatively large thermal mass attached, this might not be a significant challenge. For a 4 to 16 million pixel array, with a 20 micron pixel dimension size, this can be a significant challenge if the cooling load at the FPA varies temporally. The reasons for such variations might be either changes in incident radiation, changes in the parasitic heat gains through the optics bench, or changes in the viewing frame rate of the FPA detector system. Frame rate changes can be motivated by various target acquisition reasons; for instance, raising the rate in order to increase the amount of target data or to increase the target to clutter signal ratio in a temporal averaging algorithm. Figure 8 shows the dramatic impact of such trends in frame rate.[7]

The implications of such a change in cooling load over less than a second can be serious for any refrigeration system's thermal stability. Generally Stirling variant or Joule-Thomson refrigerators operate at 30 to 100 Hz and their control algorithms are stable with settling times on the order of minutes. Their character would therefore be unable to maintain 0.1 K thermal stability given a change in cooling load of 1 W over a second. Reverse Brayton compressor-expander output level changes would be even less responsive to such changes in FPA conditions. This indicates that serious consideration needs to be paid in future applications to how such missions can be supported using enhanced thermal interfaces between refrigerators and their supported FPAs. Such interfaces could include either phase change thermal storage devices or two phase heat transfer fluids whose interface convective transfer coefficients would be high enough to accommodate the rapid shifts in cooling load. Almost certain to be mandated by such changes in operating conditions would be the use of feed forward control algorithms to anticipate the effects of such alterations in mission requirements.

It should be noted that environmental changes for the refrigerator also have similar effects. Such changes can be caused by orbital changes in radiator view or incident radiation. Similar mitigation and control measures such as outlined above would be needed, though the radically differing time scales compared to the changes in FPA loads would indicate that distinct control algorithms would be necessary.

THE IMPACT OF REFRIGERATION SYSTEMS ON PAYLOADS

The fitting of a specific cryocooler to a potential mission is a two-step process. The FPA alternatives must be assessed to include creation of consistent figures of merit showing the relative advantages of these items. The refrigeration system needed to support each FPA must be specified in its general character, and the penalties for the potential payload estimated.[2] It can be updated for the 35 K HgCdTe versus 10 K Si:As FPA comparison.

Estimation of the payload effects of the total optical bench entailed by these FPAs considers the following issues:

- *How does the optical bench reject waste heat from the refrigeration system and what mass penalty is entailed?*
- *What is the total power budget of the refrigerator and what is the mass penalty entailed?*
- *What is the intrinsic mass penalty of the refrigerator itself, and whatever specialized linkages are specified between the refrigerator and the FPA?*

In this comparison, the usual comparative unit is that of mass, as different alternatives impose different launch masses on the entire program which is the generic cost driver for the entire program on a first run basis.

Total power draw must be converted into mass equivalents based on the efficiency of the power supply and bus. This power draw equivalent mass is then added to the mass of the radiator needed to reject this input after it has been used in the refrigeration and electronics system. If any items are mounted on a gimbal, then counterweight mass penalties must be added. To estimate these weight penalties, two examples are provided, both involving cryogenic refrigeration systems available either at present or in the next year. The first example is the Northrop Grumman High Capacity cryocooler[8] which is currently operational, and the second example is the Lockheed Martin three-stage 10 K pulse tube[9], whose cold end is currently operational and whose compressor is in prototype testing.

To simplify, with a rejection sink temperature of 300 K, the loads on the three stages in the cryostat design are specified as assumptions. For the two cases of a 10 K and 35 K cold end the loads on each stage are in Table 2. Also given are the mass penalties for supporting these systems on-gimbal. These are for a low Earth orbit with considerable radiative interaction between the Earth and the radiator and the rest of the satellite structure. For higher geosynchronous orbits there would be lower radiator penalties (on the order of 0.08 kg/W) but higher overall concern with mass as a figure of merit for the overall payload. The final simplification is the assumption that the optics mass is constant between these two payloads.

Any refrigeration system presents supported load curves like those shown in Figures 9 and 10 for the Lockheed Martin three-stage or Northrop Grumman two-stage systems. Figures 9 and 10 are valuable in that they offer the results of empirical data, but such data are not measured for all possible operating conditions. To remedy this, either interpolating models based on performance across a wide range of conditions are obtained, or models based on theoretical component interactions are validated from empirical data and then used to predict performance across the operating envelope. As an example of the latter approach, Lockheed Martin prepared explicit estimates for this study of their three-stage pulse tube's power input requirements, which resulted in requirements for power input given in Tables 3 and 4. Based on the equality of input power to the refrigeration electronics with the waste heat to be radiated and the power input required from the power bus, the appropriate mass penalties can be assessed and then totalled.

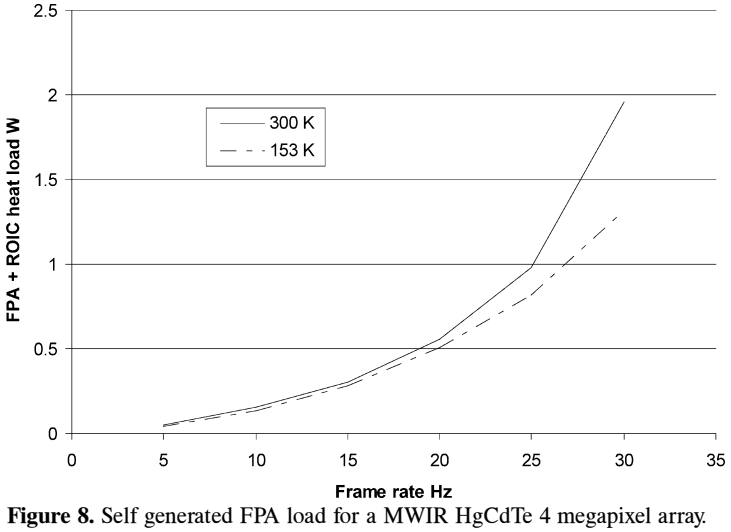

Figure 8. Self generated FPA load for a MWIR HgCdTe 4 megapixel array.

Table 2. Gimbaled refrigeration hypothetical loads and trade penalties

	10 K	35 K	LEO Penalties	GEO Penalties
85 K load	5 W	6 W		
40 K load	1.5 W			
35 K FPA load		2 W		
10 K FPA load	0.225 W			
Waste heat reject penalty			0.5 kg/W	0.08 kg/W
Power bus penalty			0.2 kg/W	0.2 kg/W
Gimbal counterweight penalty			30% of refrigerator and radiator mass	30% of refrigerator and radiator mass
Gimbal mount for cooler penalty			12 kg	12 kg

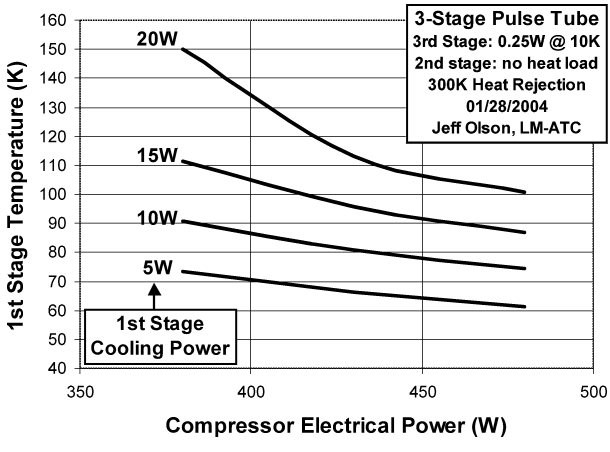

Figure 9. Typical supported cooling load trends for the Lockheed Martin three stage pulse tube (AFMHP cold end and M5MEGA compressor configuration).

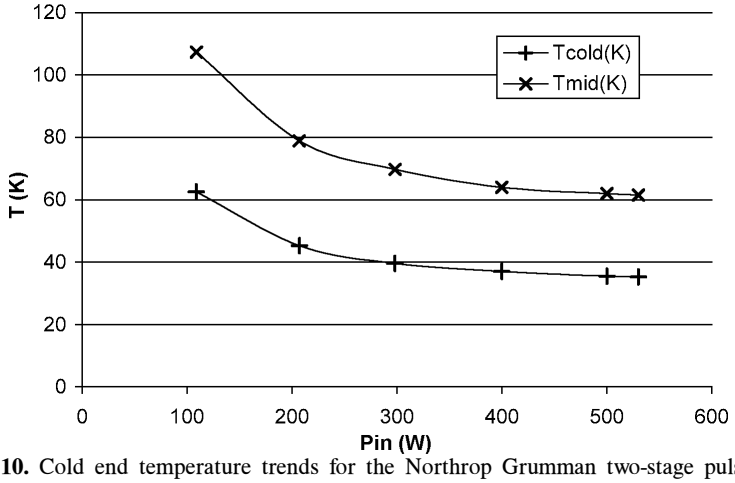

Figure 10. Cold end temperature trends for the Northrop Grumman two-stage pulse tube with simultaneous 2 W load at T_{cold} and 6 W load at T_{mid}.

Table 3. Low-earth-orbit refrigeration alternatives with mass penalties.

		Power input (W)	Refrig-erator mass-kg	Radiator mass-kg	Mount mass-kg	Counter-weight mass-kg	Power mass-kg	Total penalty in kg
LM 10 K AFMHP Coldhead	MEGA Compressor	627	18	314	12	103	125	554
	Enhanced M5MEGA Compressor	448	18	224	12	76	90	402
	Enhanced M5MIDI Compressor	693	7	347	12	110	139	607
New 3-Stage Coldhead	MEGA Compressor	535	18	268	12	89	107	476
	Enhanced M5MEGA Compressor	389	18	195	12	67	78	352
	Enhanced M5MIDI Compressor	558	7	279	12	89	112	492
NG 2 Stage 35 K								
	NG HCC	530	22	265	12	90	106	473

Table 4. Geosynchronous orbit refrigeration alternatives with mass penalties.

		Power input (W)	Refrig-erator mass-kg	Radiator mass-kg	Mount mass-kg	Counter-weight mass-kg	Power mass-kg	Total penalty in kg
LM 10 K AFMHP Coldhead	MEGA Compressor	627	18	50	12	24	125	212
	Enhanced M5MEGA Compressor	448	18	36	12	20	90	157
	Enhanced M5MIDI Compressor	693	7	55	12	22	139	228
New 3-Stage Coldhead	MEGA Compressor	535	18	43	12	22	107	184
	Enhanced M5MEGA Compressor	389	18	31	12	18	78	139
	Enhanced M5MIDI Compressor	558	7	45	12	19	112	187
NG 2 Stage 35 K								
	NG HCC	530	22	42	12	23	106	183

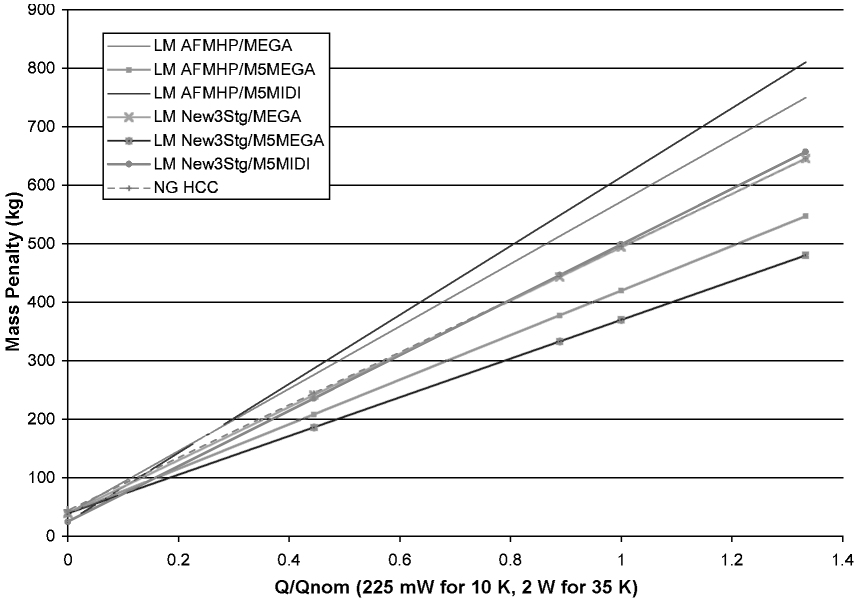

Figure 11. LEO orbit trade space results across various FPA loads, Q.

Several conclusions are apparent from a review of Tables 3 and 4. First, the actual mass of the cryocooler is an order of magnitude less in effect on payload mass than the indirect effects of the refrigeration cycle's power requirements and its waste heat rejection needs. Although this is an obvious conclusion for even modest terrestrial refrigeration applications, it applies strenuously to spacecraft payloads due to their reliance on radiative sources for power, and sinks for heat rejection.

The second conclusion that is evident is that there is no particular refrigeration advantage to a 35 K FPA, given the current status of cryogenic refrigeration and radiators. Within competitive trade spaces, the decision to use a 35 K HgCdTe FPA or a 10 K Si:As FPA should be largely based upon the merits of those FPAs. This does not preclude specific improvements in their temperature range of cryogenic refrigeration from making some specific refrigerator, FPA and associated optical bench, and payload appear marginally superior in payload trade-space for a specific application. Given the fact that the relative merits of various FPAs vary so widely depending on application, it would be wise in the future to design the FPA to the application and then design the refrigeration system to support the FPA, rather than letting refrigeration system availability decide which FPA to use.

Finally, it should be noted from the form of the penalties for each orbit that the relation between total trade-space penalty and refrigeration power input or refrigerator mass is linear. This relationship can be seen in Figure 11. This enables the restatement of this system as an under determined system of equations in matrix form for the mission payload specified and refrigeration efficiencies of the relevant refrigerators. The system for 1 through *n* orbital trade spaces is:

$$\begin{bmatrix} 1+\kappa_{cw,1} & 1+\kappa_{cw,1} & \kappa_{rad,1}+\kappa_{p,1}+\kappa_{cw,1}\kappa_{rad,1} \\ \vdots & \vdots & \vdots \\ 1+\kappa_{cw,n} & 1+\kappa_{cw,n} & \kappa_{rad,n}+\kappa_{p,n}+\kappa_{cw,n}\kappa_{rad,n} \end{bmatrix} \begin{bmatrix} m_r \\ m_{mt} \\ P_{in} \end{bmatrix} = \begin{bmatrix} m_{ttl,1} \\ \vdots \\ m_{ttl,n} \end{bmatrix} \quad (1)$$

where m is the mass, P_{in} *is* the input power, k is the trade space mass penalty factors and subscripts *r, mt, p, rad, cw, ttl* are the refrigerator, mount, power bus, radiator, counterweight, total refrigerator system, respectively.

This system keeps the elements for mount and refrigerator mass separate, as they generally can vary independently. This can be restated in terms of FPA loads and refrigeration efficiency:

$$\begin{bmatrix} 1+\kappa_{cw,1} & 1+\kappa_{cw,1} & \dfrac{\kappa_{rad,1}+\kappa_{p,1}+\kappa_{cw,1}\kappa_{rad,1}}{\varepsilon} \\ \vdots & \vdots & \vdots \\ 1+\kappa_{cw,n} & 1+\kappa_{cw,n} & \dfrac{\kappa_{rad,n}+\kappa_{p,n}+\kappa_{cw,n}\kappa_{rad,n}}{\varepsilon} \end{bmatrix} \begin{bmatrix} m_r \\ m_{mt} \\ Q \end{bmatrix} = \begin{bmatrix} m_{ttl,1} \\ \vdots \\ m_{ttl,n} \end{bmatrix} \tag{2}$$

where Q is the FPA load, e is the refrigeration efficiency, Q/P_{in} .

The Jacobian, whose ith rows are:

$$\left[\frac{\partial m_{ttl,i}}{\partial m_r} = 1+\kappa_{cw,i} \quad \frac{\partial m_{ttl,i}}{\partial m_{mt}} = 1+\kappa_{cw,i} \quad \frac{\partial m_{ttl,i}}{\partial Q} = \frac{\kappa_{rad,i}+\kappa_{p,i}\kappa_{cw,i}\kappa_{rad,i}}{\varepsilon} \right] \tag{3}$$

indicates that these trade-space surfaces are planar, and we can predict that for any two refrigerators under consideration (with their intrinsic efficiencies and FPA loads and relations) the intersection of their planar trade surfaces for any orbit represents the point at which two cooler alternatives are equivalent in total mass penalty to the payload. Above that intersection one cooler is superior and below the other is superior. In our case above, we cannot continuously scale the masses of the refrigerators themselves up and down (though the Lockheed Martin options show how this is effectively done within a design family), and mounting masses are being held constant. So FPA load is the sole independent variable for our consideration. The results of an analysis of the seven options presented in Table 3 is shown in Figure 11. Practically, the refrigerators that Table 3 indicates as optimal remain optimal until FPA loads almost disappear.

REFERENCES

1. Ross, R.G., Jr., “Aerospace Coolers: a 50-Year Quest for Long-life Cryogenic Cooling in Space,” *Cryogenic Engineering: Fifty Years of Progress*, Springer Publishers, New York, 2006.
2. Accetta, J. S. and Schumaker, D. L., eds. *The Infrared and Electro-Optical Systems Handbook, Vol. 5*, SPIE Optical Eng. Pr., Bellingham WA, 1993
3. Hubbs, J., “Radiometric Characterizations of Infrared Focal Plane Arrays (IRFPAs),” internal report, Air Force Research Laboratory, Infrared Devices Laboratory, Kirtland AFB, NM; 2005.
4. Lomheim T. S., *Infrared Imaging: Applications and Subsystems*, UCLA, Los Angeles, CA, unpublished course notes, 2006.
5. Hubbs, J., “What is a Focal Plane Array (FPA)?,” Air Force Research Laboratory, Infrared Devices Laboratory, Kirtland AFB, NM; unpublished course notes, c. 2004.
6. Lawrie, D. G. and Lomheim, T. S., *Advanced Electro-Optical Space-Based Systems for Missile Surveillance,* SMC-TR-02-15/Aerospace TR-2001(8556), The Aerospace Corporation, El Segundo, CA (2001).
7. Rockwell Scientific, *Large Focal Plane Array Technology Roadmap*, Santa Barbara, CA, 2005.
8. Jaco, C., et al., “High Capacity Staged Pulse Tube Cooler,” *Adv. in Cryogenic Engineering,* Vol. 49B, Amer. Institute of Physics, Melville, NY (2004), pp. 1263-1268.
9. Nast, T., Olson, J., Roth, E., Evtimov, B., Frank, D., and Champagne, P., "Development of Remote Cooling Systems for Low-Temperature, Space-Borne Systems," *Cryocoolers 14,* ICC Press, Boulder, CO (2007), this proceedings.